Journal of Institute of Science and Technology, 29(1), 59-73 (2024)
ISSN: 2467-9062 (print), e-ISSN: 2467-9240
https://doi.org/10.3126/jist.v29i1.66351

Research Article

LANDSLIDE SUSCEPTIBILITY MAPPING AND VULNERABILITY ASSESSMENT IN THE BADIGAD WATERSHED OF WESTERN NEPAL

Suwash Bhandari[1], Motilal Ghimire[2], Purusottam Mahat[3]

[1]Central Department of Environmental Science, Tribhuvan University, Kathmandu, Nepal
[2]Central Department of Geography, Tribhuvan University, Kathmandu, Nepal
[3]School of Environmental Science and Management, Pokhara University, Kathmandu, Nepal
[*]Correspondence: bhandariktm01@gmail.com

(***Received**: December 28, 2022; **Final Revision**: May 28, 2024; **Accepted**: June 02, 2024)*

ABSTRACT
The landslide is a major and common natural hazard in the Nepalese Himalayas. This phenomenon is because of its active tectonic setting, extensively deformed rock formation, steep mountain terrain, frequent seismic events, high-intensity rainfall during monsoons, and high rate of weathering it occurs every year, especially during the monsoon season. The landslide susceptibility assessment using the Geographic Information System (GIS) and remote sensing tools helps to display the hazards, and vulnerable zones providing the required knowledge of the susceptibility of landslides in a specific region. Landslide susceptibility with vulnerability assessment covering the comprehensive parameters provides an important understanding of the areas that are more likely to the damaging effect of the landslide hazards and is useful for mitigation, management, and avoiding threats. A total of 339 landslides were identified in the Badigad watershed from the satellite images on Google Earth, out of which 20% were used for model validation. The study was carried out using the Weight of Evidence (WoE) model. Eleven factors were considered as possible causative factors for the hazard assessment. Based on the landslide susceptibility map, 11% to 29 % of the study area is found to be in the range of very high to shallow landslide susceptibility. From the final map prepared it is found that many areas of Satyawati Rural Municipality (RM), Ruru RM, Chandrakot RM, and Chhatrakot RM, along with Musikot Municipality in Gulmi and Badigad RM in Baglung district, exhibit a notable high hazard level. The Receiver Operating Characteristics (ROC) graph with the Area under the curve (AUC) value was used to check the performance of the WoE model which shows that the model has 80.4% prediction accuracy for future events which means, the model shows very good performance. The vulnerability within the study area is assessed by obtaining vulnerability scores. To obtain the vulnerability score, fourteen indicators were analyzed following the Local Disaster and Climate Resilience Planning (LDCRP) guideline. The result obtained from the vulnerability assessment showed that two wards, namely Thulolumpek in Satyawati RM of Gulmi and Bobang in Dhorpatan Municipality of Baglung are highly vulnerable. By analyzing and comparing the vulnerability obtained from susceptibility mapping (using GIS) and social methods (using LDCRP guideline), it is observed that they do not converge based on the factors studied.

Keywords: Area under curve, Badigad watershed, landslide susceptibility, vulnerability, the weight of evidence

INTRODUCTION
Landslide, a synonym of the terms like "mass movement", and "slope movements", is the movement of rocks, debris, or earth materials down the slope (Cruden, 1991). The basics of landslide causes, locations, forms, mechanisms, and processes were reported by several scientific studies on Nepal Himalaya (Hasegawa *et al.*, 2008; Dahal, 2012; Van Tien *et al.*, 2021; Singh *et al.*, 2022). Seismic activity, fragile geology, high-intensity rainfalls and weathering, and toe erosion make Nepal highly vulnerable to landslides (Baruwal, 2014). Additionally, human-induced actions, such as improper land use, intrusion into susceptible land slopes, and poorly planned development activities like constructing roads and irrigation canals without sufficient safeguards in mountainous areas, further exacerbate the likelihood of landslide occurrence (Acharya *et al.*, 2017). This heightened risk contributes to human and infrastructure losses in the mountain and hilly areas especially during the monsoon (Petley *et al.*, 2007). Every year a total of about 12,000 small and large-scale landslides occur in Nepal most of which often remain ignored and unreported mainly because of an inadequate information system, little economic impact, or little harm to humans and national infrastructure (Bhattarai *et al.*, 2002). Despite their often-overlooked nature, landslides alone are responsible for causing annual human deaths of over 300 in Nepal (Hearn *et al.*, 2003). Consequently, there is a critical need to conduct landslide susceptibility mapping to identify the potential landslide areas.

Landslide susceptibility is the tendency or preference to answer where the future landslide can occur over an area without explaining the exact time of occurrence and intensity (Rabby & Li, 2020). It is based on the assumption that "the past is the key to the future," where historical landslides and their relationship with causative factors can be used to predict future events (Van Westen *et al.*, 2008). Various methods, including statistical techniques (Mersha & Meten, 2020), deterministic analyses, and heuristic approaches (Zorgati *et al.*, 2019), can be employed to create landslide susceptibility maps.

However, all these methods are not equally taken in landslide mapping and analysis due to technical and cost constraints (Soeters & Van Westen, 1996). For assessing landslide susceptibility over a large area, statistical methods are typically favored because they offer prediction without requiring the detail and extensive data for parameterizing and assessing physically based approaches (Woodard *et al., 2023).* In contrast, deterministic analysis in landslide susceptibility involves slope stability models by calculating the factor of safety in individual slopes which requires detailed geometrical data, angle of friction, and pore water pressure (Terlien *et al.,* 1995; Aleotti & Chaudhary, 1999; Regmi *et al*., 2014). Therefore, this method is normally applied only in small areas at detailed scales. Heuristic approaches are employed using ranking methods based on experts' opinions and experience (Zhu et al., 2018), including methods such as the Analytical Hierarchical process (AHP) (Abedini *et al*., 2017), and the fuzzy logic approach (Kayastha *et al*., 2012). A significant drawback of this approach is its dependency on subjective judgments which leads to the failure to quantify the importance of each factor (Chen & Song, 2023). Despite their differences, all these approaches use GIS tools, which are suitable tools for Landslide susceptibility mapping.

Landslide susceptibility mapping activities determine the areas prone to landslides based on various causative factors (Dou *et al*., 2015; Roy & Saha, 2019) while vulnerability assessment evaluates the potential damage and loss of life from extreme natural events suggesting the best-engineered approach to hazard reduction (Cutter, 1996). In the field of disaster risk reduction planning, it is essential not only to conduct landslide susceptibility mapping using the GIS tool but also to assess the vulnerability of the community by evaluating the community's exposure, sensitivity, and adaptive capacity to landslides via an integration approach (Rahman *et al.,* 2022). Vulnerability is the probability that a human-environmental system, or any one of its components, is likely to experience damage as a result of exposure, sensitivity, and adaptive capacity to hazard (Turner *et al*., 2003; Cannon, 2006; Fussel, 2007). Vulnerability assessment embraces the inherent qualities and conditions of the community, system, or asset that make it susceptible to the detrimental effects of hazards. Unfortunately, there is no universal method for assessing vulnerability across various locations and hazard levels (Papathoma-Kohle *et al*., 2007). However, according to several kinds of literature, vulnerability assessment of the community involves a method based on the integration of physical, social, and environmental aspects (Glade, 2003; Arrogante-Funes *et al*., 2021; Nor Diana *et al.,* 2021). The research conducted by Arrogante-Funes *et al*., (2021) on landslide socio-economic vulnerability assessment involves the integration method that incorporates data from the marginalization index, population density, and building density by collecting data from different sources. Similarly, the study conducted by Banuzaki & Ayu (2021) utilized a GIS tool for landslide vulnerability assessment. The methodology employed in assessing vulnerability assessment in this research aligns with the guidelines outlined in the LDCRP framework developed by GoN to comprehensively assess the communities' vulnerability to the landslides, providing insight into the degree of vulnerability they face.

The main rationale beyond this is that the study of the landslide susceptibility and vulnerability assessment within the Badigad watershed, encompassing mostly the parts of Gulmi and Baglung districts (The District is the geographical administrative area greater than municipalities, and smaller than provinces) has not been still carried out. Paudyal and Maharjan (2022) studied landslide susceptibility in the Tinau-Mathagadi section of the Palpa district using the Frequency Ratio method, and Budha *et al.,* (2020) studied the landslide susceptibility map of the Panchase area covering the parts of the Kaski, Parbat, and Syangja district. However, no study has specifically focused on landslide susceptibility including the vulnerability assessment in the Badigad watershed. This area experienced a significant loss of life due to a massive landslide in 2019 in Gulmi, resulting in 13 fatalities, and 2020 in Baglung, resulting in 14 fatalities. The main purpose of this study is to prepare the landslide susceptible map in a GIS environment which can predict the probability of potential landslide occurrence over an area in the future. Additionally, the study aims to assess the vulnerability of the wards under the study by analyzing the potential impact of loss from the event in the human-environment system. This, in turn, assists the concerned authorities in developing suitable land use planning to mitigate the occurrence of disaster and its impacts aiming to foster the resilience of vulnerable communities.

MATERIALS AND METHODS

Study area

The Badigad watershed is selected as the study area as shown in Fig. 1. It is mostly located in the western part of Nepal in the Baglung and Gulmi districts under the Lesser Himalaya covering an area of 1965 km^2 whose altitude ranges from 415 m to 3985 m. The Badigad River is a major tributary of the Kaligandaki River.

The Badigad watershed predominantly comprises 22 local governments (here, local government refers to the municipalities divided administratively) from Baglung and Gulmi districts, including 5 municipalities and 17 rural municipalities covering major residential areas like Burtibang, Hatiya, Kharbang, Wamitaksar, Bhuwachidi, Majuwa, Shantipur, Khaireni and Rudrabeni. Local government refers to the institutional units responsible for governing defined territories within the country (Acharya, 2018). Local government constitutes the wards (the smallest unit of the local government). The primary drainages in the study area include Chaldi Khola, Hugdi Khola, Gidi Khola, Bharse Khola, Lumdi Khola, Daram Khola, Taman Khola, Nisi Khola, and Bhuji Khola. Additionally, this watershed extends into the minor parts of other districts like Arghankhanchi, Pyuthan, Rukum, Rolpa, and Myagdi.

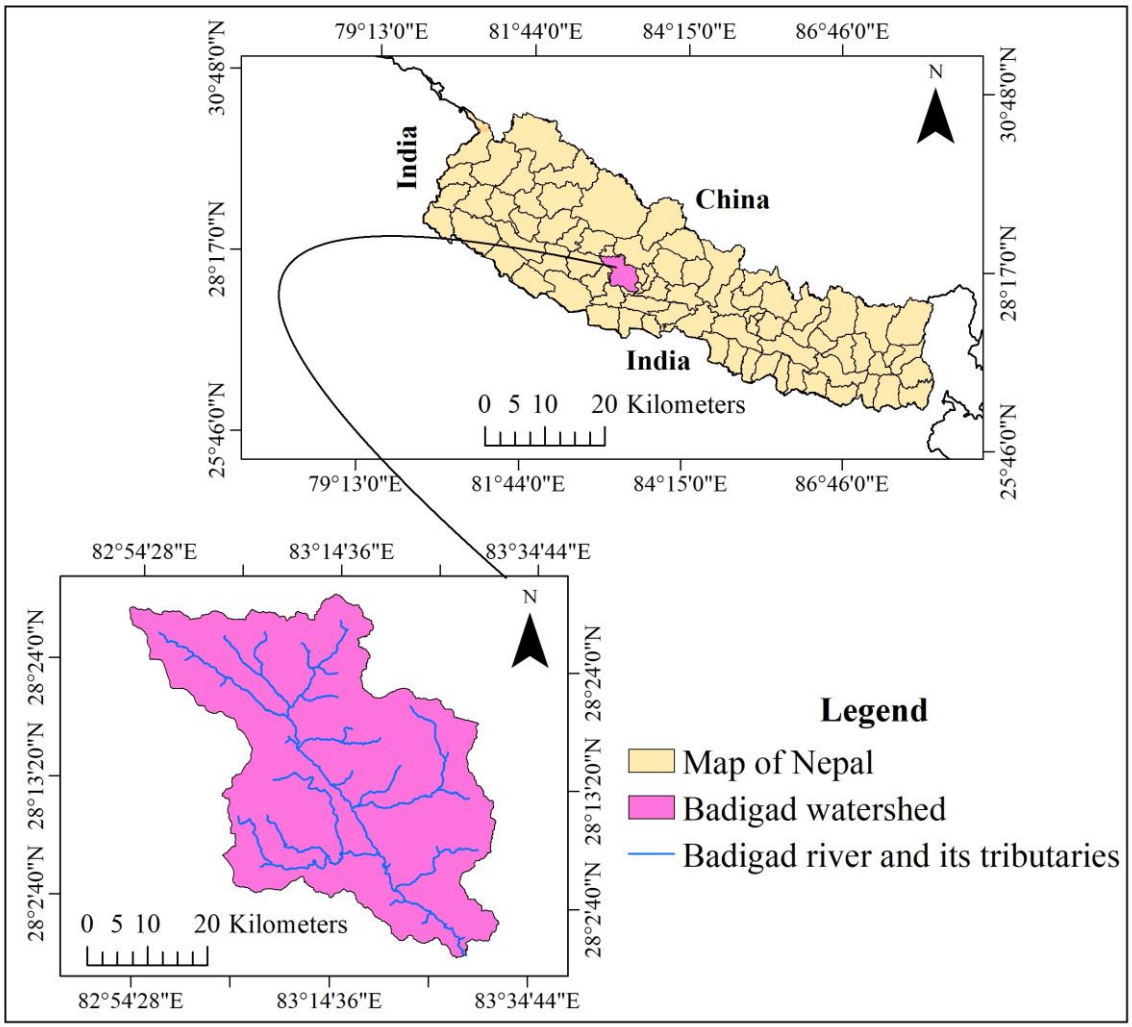

Figure 1. The Study area map (Badigad watershed)

Data preparation for landslide susceptibility

Landslide inventory is the most important step in landslide susceptibility mapping, and this includes:

- Identifying and interpreting landslide distribution through Google Earth was carried out. Landslides are identified from satellite images with the help of many attributes including color, tone, surface roughness, and texture (Mihir & Malamud, 2014).
- A Field visit for the verification and recognition of the inventoried landslide was conducted. The Global Positioning System (GPS) locations recorded on the field are subjected to Google Earth for verification.

Factors for landslide susceptibility assessment

This study utilizes ArcGIS 10.3 to map landslide susceptibility by considering various factors expected to contribute to potential future sliding based on the literature review. These factors include slope, elevation, aspect, profile and plan curvature, relief, geology, distance from the road, distance from the river, land use, and rainfall.

Landslide susceptibility assessment

In this process, the total landslide invented through Google Earth was randomly selected using the ArcGIS tool in training and testing data. Training data occupies 80% of the entire landslide data to operate the weight of the evidence model thereby generating a Landslide susceptibility map, whereas the remaining data are the testing data employed to test the model's prediction capability for the future event. Specifically, to evaluate the landslide susceptibility map generated from the model used. In this study, the Bivariate statistical analysis method known as the Weight of Evidence (WoE) Model was used, which is a data-driven approach that utilizes a log-linear variation of Bayesian analysis, operating on the basis that future landslide occurrences will occur due to the factors akin to those that led to the past landslides (Getachew & Meten, 2021). WoE involves computing

two fundamental parameters: positive weight (W^+) and negative weight (W^-), which analyze the spatial relationship between the causative factors and the distribution of landslides (Pamela *et al.*, 2018). This is achieved by overlaying the landslide inventory map with individual causative factor maps to establish spatial statistical correlations (Cao *et al.,* 2021). The positive (W^+) and negative (W^-) weight values are determined by the following equation.

$$W^+ = \ln \frac{\frac{Npix1}{Npix1+Npix2}}{\frac{Npix3}{Npix3+Npix4}} \quad \dots (1) \qquad \text{and } W^- = \ln \frac{\frac{Npix2}{Npix1+Npix2}}{\frac{Npix4}{Npix3+Npix4}} \quad \dots (2) \text{ (Van Westen, 2002)}$$

Where Npix1 is the number of pixels representing the presence of both potential landslide predictive factor and landslides, Npix2 is the number of pixels representing the presence of landslides and absence of potential landslide predictive factor, Npix3 is the number of pixels representing the presence of potential landslide predictive factor and absence of landslides, Npix4 is the number of pixels representing the absence of both potential landslide predictive factor and landslides.

The final weight is then calculated as
$Wmap = W^+ + \Sigma W^- - W^-$ … (3).

According to Bonham-Carter (1994), the spatial association between the map class and the occurrence of landslide can be calculated as:
Contrast factor (C) = $W^+ - W^-$ … (4)

The resulting total weights directly indicate the importance of each factor. If the total weight is positive, the factor is favorable for the occurrence of landslides, and if it is negative, it is not favorable.

The weightage values of all factor classes were combined using the formula below to Figure out the Landslide Susceptibility Index (LSI) map of the study area where N is the total number of factor maps (Sifa *et al.*, 2020).

$$LSI = \sum_{i=1}^{N} Wmap \quad \dots (5)$$

Finally, the preparation of the susceptibility map was carried out by integrating various factor maps stored in raster format, each assigned with specific weights. The susceptibility map was then classified into different classes of susceptibility; very low, low, medium, high, and very high based on the natural break classification method in ArcMap. Later on, this susceptible map prepared from the WoE model was verified by the ROC AUC graph by calculating the prediction rate.

Vulnerability Assessment

This assessment utilized the Local Disaster and Climate Resilience Planning (LDCRP) guideline, developed by the Government of Nepal (GoN), which incorporates 14 diverse indicators covering physical, economic, social, and environmental aspects. In this research, twenty wards within the watershed were visited based on previous landslide events to carry out vulnerability assessment using LDCRP indicators. Data for all of the indicators mentioned in the guideline were gathered through direct observation, Key Informant Interviews (KII), Focus Group Discussions (FGD), and existing published data. Each of the indicators was assigned a specific score as outlined in the guideline, and these scores were summed up to calculate the total score of the individual ward. This total score was then used to classify the vulnerability of the wards into high, medium, and low categories based on the guidelines' instructions. The scoring methods for each indicator, as recommended by the guideline, are presented in Table 1.

Table 1. Indicators and the methods of assigning scores using LDCRP guideline

S.N.	Indicators for Vulnerability Assessment	Methods of assigning scores	Score
1	Human death	0 to 1 people died = low	2
		2 to 5 people died = Medium	4
		more than 5 people died = High	6
2	Impacted households	50 Households = low	1
		51 to 100 Households = Medium	2
		Greater or equal to 101 = High	3
3	Damaged houses	0 to 10 damaged houses = low	1
		11 to 50 damaged houses = medium	2
		More than 50 damaged houses = high	3
4	Economic loss	0 to 1 lakhs = low	1
		1 to 50 lakhs loss = medium	2
		More than 50 lakhs = high	3
5	Agricultural and forest area loss	5 *Bigha* land loss = low	1
		5 to 50 *Bigha* land loss = medium	2
		More than 50 Bigha land loss = high	3
6	Social impact	Occurrences of any one of the events among disappearance of people, children, cases of violence against women, cases of robbery, or any other incident = low	1

		Occurrences of any one of the events among disappearance of people, children, cases of violence against women, cases of robbery, or any other incident = medium	2
		Occurrences of all of the events such as the disappearance of people, or children, cases of violence against women, cases of robbery, or any other incident = high	3
7	Disastrous events in the past	1 to 2 disastrous events occurred = low	1
		2 to 5 disastrous events occurred = medium	2
		More than 5 disastrous events occurred = high	3
8	Changes in the season calendar	Changes occurred within less than 10 days = low	1
		Changes occurred within 10 to 20 days = medium	2
		Changes occurred within more than 20 days = high	3
9	Changes in temperature	Only felt = low	1
		felt but less impact = medium	2
		Extinction of crops and vegetation= high	3
10	The future effect of the risk	The population of Settlements near river and landslide is Less than 10 percent = low	1
		Settlements having excessive or shortage of water, no proper management of sewage, or the population of settlements near river and landslide is Less than 10 to 30 percent = medium	2
		Settlements having excessive or shortage of water, no proper management of sewage, or the population of settlements near rivers and landslides is Less than 10 to 30 percent = high	3
11	Access to resource availability	Adequate and accessible resources = low	1
		Adequate but not accessible resources = medium	2
		Shortage of resources = high	3
12	Institutional capability	The presence of an organization that is capable of working during disastrous events = low	1
		The presence of an organization that is not capable of working during disastrous events or communities are not informed about the organization = medium	2
		The organization is too far away or there is no organization at all = high	3
13	Access to population analysis	If less than 20 percent of the population constitutes disabled persons, pregnant women, children below 5 years, and elderly people over the age of 60 = low	1
		If 20 to 40 percent of the population constitutes disabled persons, pregnant women, children below 5 years, and elderly people over the age of 60 = medium	2
		If more than percent of the population constitutes disabled persons, pregnant women, children below 5 years, and elderly people over the age of 60 = high	3
14	Knowledge, skill, capacity, and technology	Availability and Use of local knowledge, skills, abilities, and technology to minimize the effects of disasters and climate change = low	1
		Availability of local knowledge, skills, abilities, and technology to minimize the effects of disasters and climate change but not in use = medium	2
		No availability of skill, abilities, and technology = high	3

Source of Data for Landslide Susceptibility Mapping

The different data sources that were used for mapping different factors for developing landslide susceptibility are tabulated in Table 2. The PALSAR (Phased Array type L-band Synthetic Aperture Radar), Digital Elevation Model (DEM) data was used in this research which was extracted and downloaded from the Alaska Satellite Facility (ASF) having spatial resolution (Size of the smallest feature that can be detected by a satellite sensor) of 12.5 m.

Table 2. Source of data used

S.N.	Factors	Data	Source and Spatial Resolution
1	Slope	DEM	PALSAR/12.5m
2	Elevation	DEM	PALSAR/12.5m
3	Aspect	DEM	PALSAR/12.5m
4	Profile curvature	DEM	PALSAR/12.5m
5	Plan curvature	DEM	PALSAR/12.5m
6	Relief	DEM	PALSAR/12.5m
7	Geology	Geological formation	Department of Mines and Survey, 2020
8	Distance from Road	Road	Open street map, 2020
9	Distance from River	DEM	PALSAR/12.5m
10	Land Use	Satellite image (Landsat 8)	United States Geological Survey, 2020
11	Rainfall	Annual rainfall data	DHM Nepal, 2020

RESULTS AND DISCUSSION

Landslide Inventory Map

Using the Google Earth image, a total of 339 landslides from the year 1985 to 2021 are mapped where landslides are located very near to the confluence of the Badigad River and its drainage network, on the middle slope and in the foot slope close to the river. Out of the total mapped landslides, 80% were randomly selected using the GIS tool as a training sample for the mapping and analysis by running the model while remaining of the landslides mapped were testing landslides as shown in Fig. 2. These testing landslides were employed to assess the accuracy of the model through which the susceptible map is prepared.

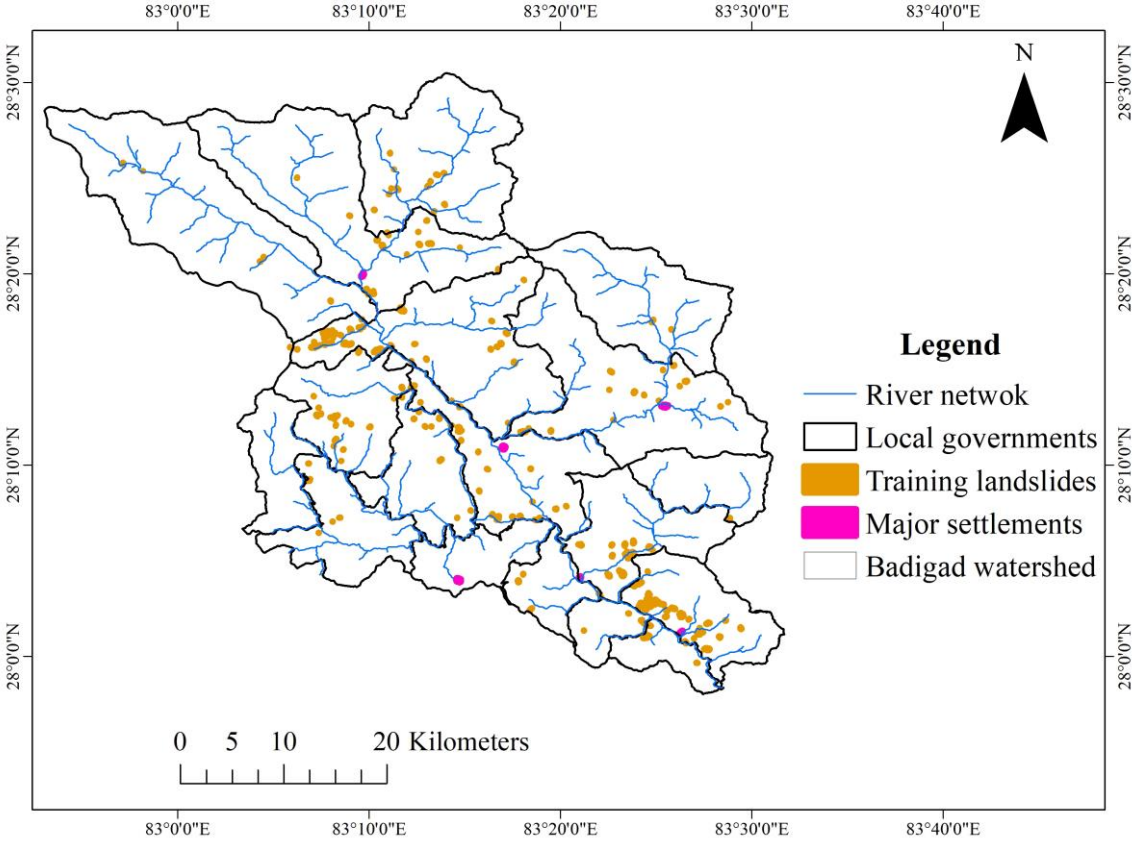

Figure 2. Landslide inventory map showing the distribution of landslides

Factor maps and the weighted values

Factor maps are thematic maps that represent the different causative variables contributing to the likelihood of landslides occurring in a specific area. There is no standard or guideline for selecting the factors in landslide susceptibility mapping (Ayalew & Yamagishi, 2005; Sato & Harp, 2009). However, the causative factors in this study were taken into account from the literature review. All of the factor maps considered in this study were categorized into distinct classes within a GIS, assigned with weightage values (W^+ and W^-). Subsequently, W_{map} and contrast were calculated and tabulated in Table 3 to assess the individual contributions of each factor class to the spatial occurrence of landslides.

The weightage values computed using the WoE model as shown in Table 3 are crucial for understanding the significance of each factor class in landslide occurrence. A brief description of the results of each evaluated thematic map in this study is given below.

The Slope factor is the most significant in the occurrence of landslides as it affects the soil water content (surface and subsurface), formation of soil, erosion potential, and so on (Poudel & Regmi, 2016). Among the four different classes of slope, as shown in Fig. 3a, the slope class of 30-45° has the maximum positive weightage and contrast value identical to Thapa and Esaki (2007) and differs from that of Kayastha *et al.* (2012, 2013) and Sarkar *et al.* (2006). This particular slope class predominately features major cultivated lands and grasslands devoid of trees, thus increasing the likelihood of landslides.

Table 3. Weighted value for each factor class

Factors	Class	No. of pixels of landslides	No. of the pixel of subclass	W_{map}	Contrast
Slope (°)	<15°	291	1053632	-1.68	-1.3
	15-30°	2942	4751905	-1.00	-0.62
	30-45°	7026	5556404	0.21	0.59
	>45°	1671	1215271	0.04	0.42
Elevation (m)	<1000	5157	1193376	1.88	1.99
	1000-1500	4275	3447560	0.29	0.39
	1500-2000	2031	3194481	-0.61	-0.51
	2000-2500	409	2582545	-2.09	-1.99
	>2500	58	2159250	-3.85	-3.75
Aspect	Flat	2	3639	-0.58	-0.54
	North (N)	480	1585507	-1.24	-1.24
	Northeast(NE)	224	1488117	-1.95	-1.95
	East (E)	399	1492505	-1.36	-1.43
	Southeast (SE)	1953	1656600	0.25	0.31
	South (S)	2376	1709657	0.45	0.46
	Southwest (SW)	2546	1763137	0.50	0.51
	West (W)	2255	1411006	0.61	0.61
	Northwest (NW)	1712	1443256	0.25	0.26
Profile curvature	Convex	3003	2159702	0.14	0.10
	Planar	6134	6969632	-0.12	-0.16
	Concave	2793	3447878	-0.17	-0.21
Plan curvature	Concave	10607	2135828	0.57	0.48
	Planar	670	8226328	-0.18	-0.26
	Convex	608	2215056	-0.04	-0.13
Relief (m)	< 50	295	1605193	-1.78	-1.74
	50-70	1171	2441753	-0.82	-0.78
	70-100	4695	4470397	0.14	0.18
	100-120	3090	2216738	0.46	0.50
	>120	2679	1964875	0.42	0.46
Geological Formation	Lakharpata	2332	3543541	-0.56	-0.48
	Siuri	1276	1493809	-0.2	-0.12
	Kushma	15	325634	-2.75	-2.68
	Galyang	5173	110097	1.65	1.73
	Syangja	1961	225495	-0.21	-0.13
	Ranimatta	994	1505769	-0.83	-0.75
	Sangram	183	2299661	-1.83	-1.75
	Seti	0	2036107	0	0
	Surbang	0	1038146	0	0
Distance from road (m)	< 50	1418	114997	0.31	0.29
	50 – 100	720	906519	-0.17	-0.19
	100 – 150	559	755887	-0.25	-0.26
	150 – 200	548	650435	-0.11	-0.12
	200 – 250	685	575627	0.25	0.24
	250 <	8000	8539286	-0.02	-0.03
Distance from river (m)	< 40	596	762608	-0.03	-0.21
	40 – 80	939	740977	0.48	0.31
	80 – 120	1072	715380	0.66	0.49
	120 – 160	983	703128	0.59	0.42
	160 – 200	853	679854	0.47	0.29
	200 <	7487	8975304	-0.22	-0.39
Land use	Agriculture	7039	4170290	0.32	-0.31
	Forest	3377	7031434	-0.02	-0.02
	Built-up	1970	449	0	0
	Grassland	232	1209944	0.54	0.54
	Barren land	96	42260	1.71	1.71
	Waterbody	0	113841	-0.16	-0.18
Rainfall (mm)	<1800	5956	1513045	1.88	1.99
	1800-2000	1812	2844062	-0.60	-0.49
	2000-2200	1185	2324665	-0.83	-0.72
	2200-2400	821	2798047	-1.46	-1.35
	>2400	2156	3097432	-0.50	-0.39

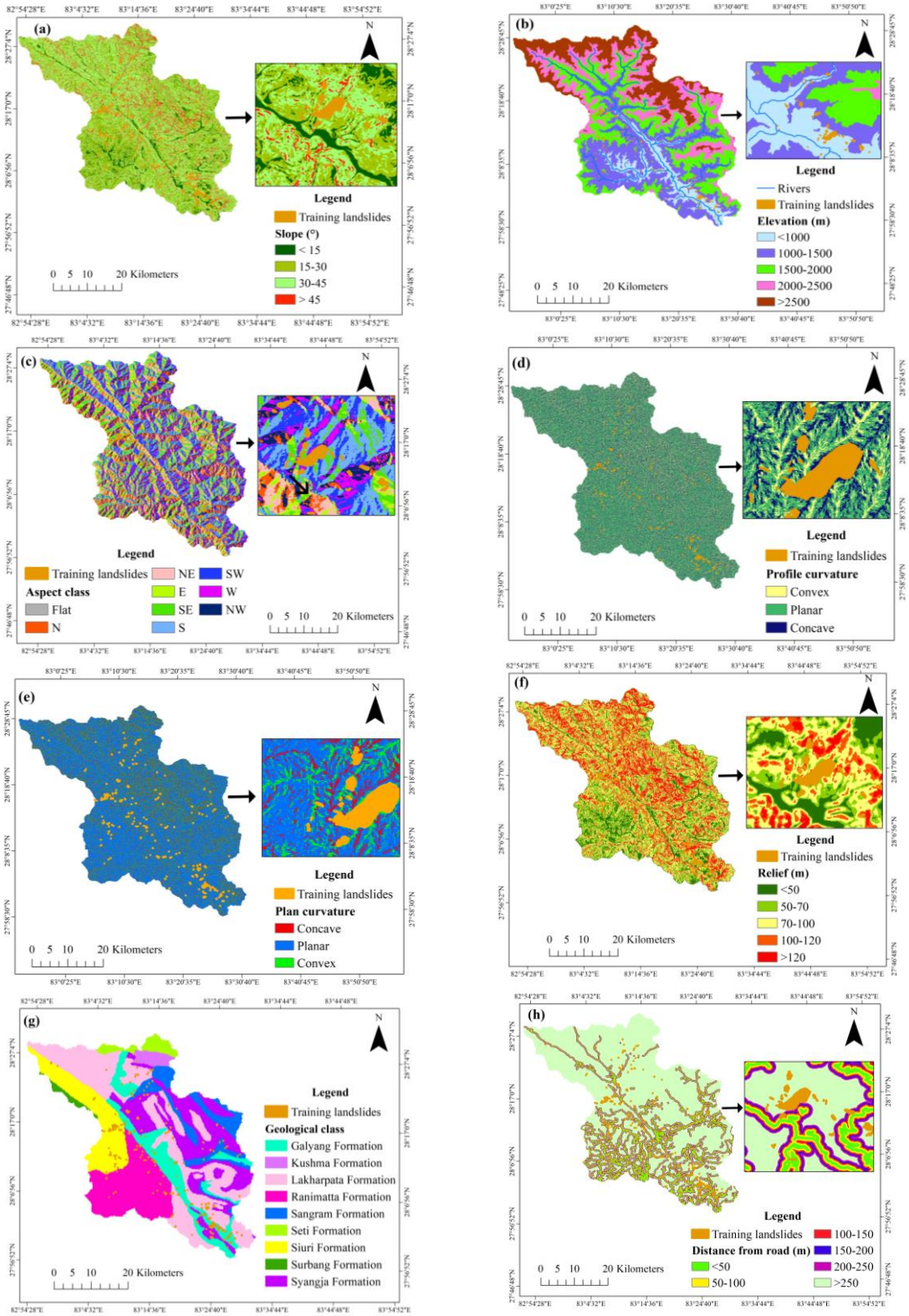

Figure 3. Landslides in each class of (a) Slope (b) Elevation (c) Aspect (d) Profile curvature (e) Plan curvature (f) Relief (g) Geology and (h) Distance from road

The elevation was categorized into five classes as shown in Fig. 3b. Within these categories, the possibility of landslides occurring is found to be maximum in the elevation class of <1000m, followed by the range of 1000-1500 m while is minimum in elevation exceeding 2500 m (Table 3). According to Ghimire (2011), there is no significant relationship between the elevation and landslides alone, however, elevation is linked with other parameters like aspect, and slope shows a significant association for causing landslides.

The aspect map of this study area was derived from the DEM data and categorized into nine classes as shown in Fig.3c. Majority of landslides in the aspect class are likely to occur in west and south-facing slopes in this study area with positive weightage value. This is probably due to the prevailing direction of monsoon storms that enter through the southeast and slowly move towards the Northwest resulting in a lot of precipitation on the south and west-facing slopes similar to the study conducted by Kayastha *et al.* (2012).

In this study, the profile and the plan curvature were used and classified into three classes, namely, concave, planar, and convex as shown in Fig 3d and 3e. Convex of profile curvature and concave of plan curvature and has the highest probability of occurring landslides in the study area. It is because concave curvatures effectively preserve water for a longer period favorable for landslides whereas external forces like weathering of rocks, pore water pressure, infiltration of rainwater, etc. in a convex slope lead to its failure. Convex curvature is more susceptible to landslide (Lee & Pradhan, 2007) while Regmi *et al.* (2014) concluded that concave curvature is more susceptible to landslide occurrence. Hence, the curvature is more responsible for triggering landslides.

The relief factor of the landslide susceptibility was reclassified into < 50m, 50-70m, 70-100m, 100-120m, and >120 as shown in Fig. 3f. The probability of event occurrence is likely to happen in the relief class of 70-100 m, 100-120 m and greater than 120m. It may be due to the disorderly built road construction activities under the relief class favorable to landslides.

In this study, geological data was classified into 9 classes based on geological formations as shown in Fig. 3g. The Galyang formation is found to have positive weightage and contrast values, as tabulated in Table 3, indicating a higher probability of slope failure within this class. This geological formation primarily comprises olive green, brown, and gray phyllite grey siliceous dolomites, grey slates, and phyllitic quartzites (Ojha, 2009; Robinson & DeCelles, 2014). This composition contributes to an increased susceptibility to landslide due to its high rate of weathering and erosion.

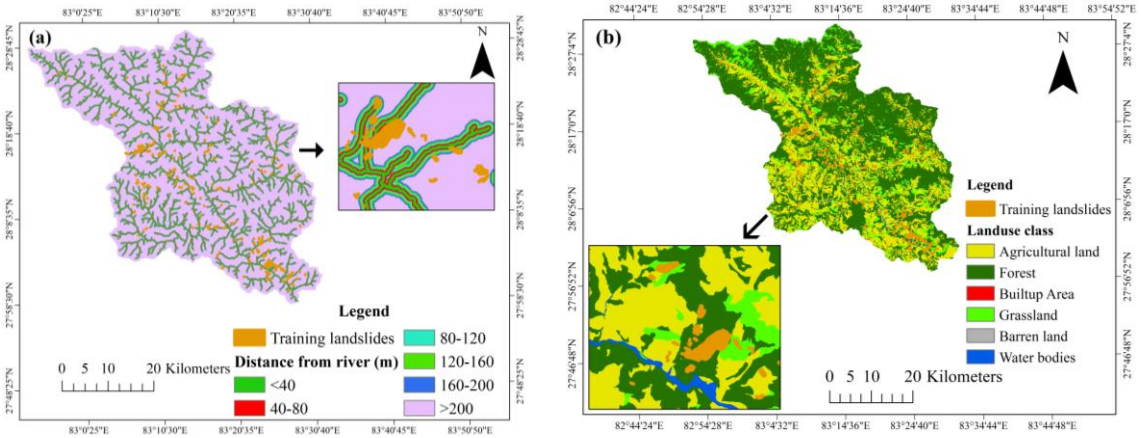

Figure 4. Landslides in each class of (a) Distance from river (b) Landuse

The distance from the road factor is categorized into <50m, 50-100m, <100-150m, 150-200m, 200-250m, and >250m as shown in Fig. 3h. The weightage value is calculated to be positive in the class very close to the road i.e. < 50 m distance. This indicates the probability of landslide occurrence along the roadside is maximum because the road construction activities destabilize the slope by cutting down vegetation (Dahal, 2017). The weightage value decreases while going farther from the road having a lesser probability of event occurrence similar to the study conducted by (Regmi *et al.,* 2014).

The distance from the river was reclassified into six classes with 40m intervals: <40m, 40-80m, 80-120m, 120-160m, 160-200m, and >200m (Fig. 4a). Negative weightage and contrast value is observed in the class very closer to the riverside which signifies the occurrence of the landslide is in decreasing way as the event occurred place is farther from the river. This suggests other factors than the distance from the river is responsible for landslide occurrence consistent with the study performed by (Getachew & Meten, 2021) in their study area.

The land use map in this study was classified into six classes, namely, agricultural land, forest, built-up area, grassland, barren land, and water bodies (Fig. 4b). The possibility of the occurrence of landslides was found in grassland and barren land. The barren land and grassland lacking plant roots could not stabilize the soil and rock leading to the landslide failure. The study conducted by Kayastha (2012) found barren land as the most susceptible areas while Gerrad and Gardner (1999) found grassland as highly susceptible areas.

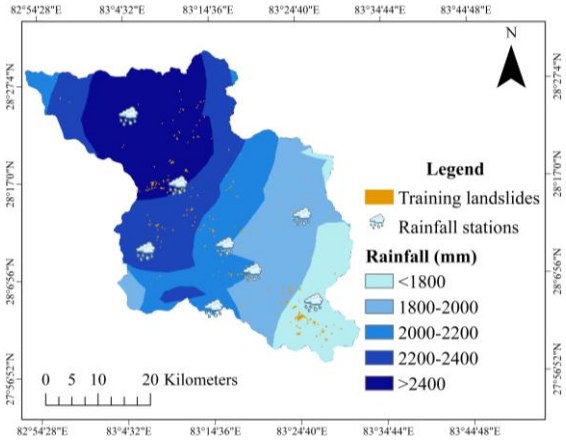

Figure 5. Landslides in each class of rainfall

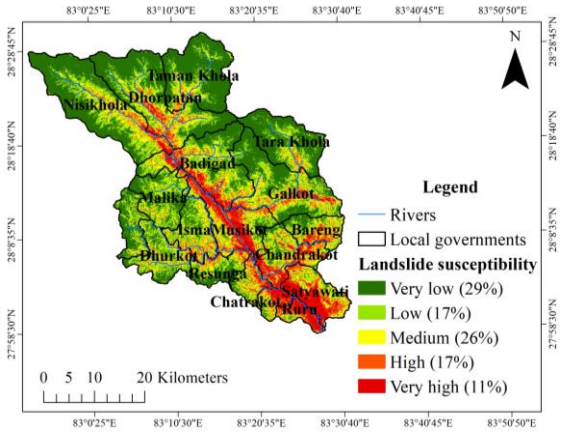

Figure 6. Landslide susceptibility map based on WoE model

In this study, a negative correlation between the amount of precipitation and the landslides is found to be maximum in the class 2200-2400 mm. It may be due to the strength of materials on the slope like solid rocks which cannot be easily eroded by prolonged rainfall. However, high intensity of rainfall may make such areas susceptible to the event. In addition, some uncertainties in the data provided by the Department of Hydrology and Meteorology (DHM) may have resulted in unexpected outcomes in this factor. The spatial distribution of landslides in different classes of rainfall is shown in Fig. 5.

Landslide susceptible map

The landslide-susceptible map is produced by using the WoE method based on the weighted value from the eleven causative factors and the training landslides. The LSI values for the WoE model were prepared by the summing W_{map} of all the factors considered whose values range from 10 to -13. This range of values was categorized into five different susceptibility zones using the natural break classification method in ArcMap. The five susceptibility zones include very low, low, medium, high, and very high classes comprising 29%, 17%, 26%, 17%, and 11% respectively as shown in Fig.6. In this study, the WoE model shows that there is greater significance of plan curvature, land use and land cover and distance from road in the occurrence of the landslide. Based on the landslide susceptible map prepared, many areas of Satyawati Rural Municipality (RM), Ruru RM, Chandrakot RM, and Chhatrakot RM including Musikot Municipality of Gulmi and Badigad RM of Baglung district are observed to be very high hazard.

Model Validation

The Receiver Operating Characteristics (ROC) graph with Area under Curve (AUC) value is widely used to evaluate the performance of the model used in landslide hazard and susceptibility analysis (Dahal et al., 2012; Wang et al., 2016; Nohani et al., 2019; Zhao & Chen, 2020). In this study, the evaluation process involves the creation of the prediction rate curves from testing data. The AUC value of the predictive rate curves was used for the evaluation of the landslide susceptibility map which explains how well the model used can predict future or upcoming events. AUC values equal to or below 0.5 suggest ineffective prediction or no improvement, whereas values equal to or above 0.7 indicate the excellent prediction of the model in landslide susceptibility (Devkota *et al., 2013)*. The prediction rate curve in this study showed 0.804 AUC value which means the model had predictability of 80.4%, indicating very good performance of the model in landslide prediction in the study area (Fig. 7). The study conducted by Budha *et al.* (2016) found that there is 0.76 AUC in their model validation that means the model had predictability of 76% (good performance of the model in landslide prediction) in eastern hills of Rara lake western Nepal.

The guideline of LDCRP with 14 different indicators is followed for vulnerability assessment. Scores are assigned to each indicator according to the criteria outlined in the guidelines during the data collection process. Based on the guideline the collected scores for each indicator are summed up to obtain the total score from which the vulnerability class is separated and tabulated in Tables 3 and 4.

Most of the area in the study site was found to have medium vulnerability because of the improving economic status of the people as consistent with the research conducted by Glade (2003) in his study area. The only wards taken for assessing vulnerability under this study were classified into three different classes: highly vulnerable, medium vulnerable, and low vulnerability class represented by red, green, and blue colors respectively as shown in Fig. 8. These wards were chosen for the vulnerability assessment based upon the past landslide event.

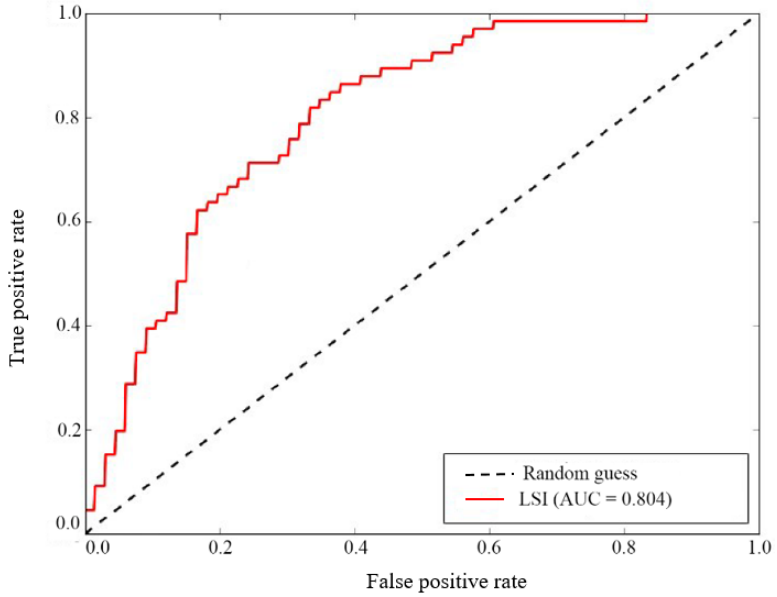

Figure 7. ROC graph to validate the model used

Table 3. Local administration and their wards under study

S.N.	District	Local Administration	Ward Number	No. of wards	Scores
1	Gulmi	Satyawati RM	3, 4 and 6	3	39,36 and 28
2	Gulmi	Chandrakot RM	7 and 8	2	33 and 23
3	Gulmi	Musikot Municipality	2,3,5,6 and 8	5	30,31,38,35 and 34
4	Baglung	Badigad RM	4,5,7,8 and 9	5	34,34,31,31 and 30
5	Baglung	Dhorpatan Municipality	5,6,7,8 and 9	5	35,38,34,38 and 39
				Total=20	

Table 4. Vulnerability class based on LDCRP guideline

S.N.	Vulnerability score	Vulnerability Class
1	< 24	Low
2	24-38	Medium
3	38-39	High

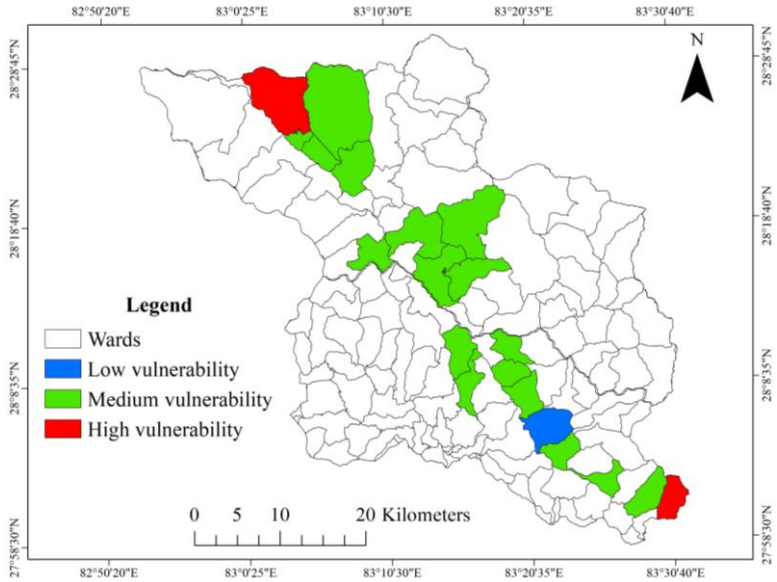

Figure 8. Vulnerability map created following the LDCRP guideline

The Bobang of Baglung (Dhorpatan-9), and Thulolumpek (Satyawati-3) area of Gulmi is found to be highly vulnerable (Fig. 8). This is because the landslides have highly affected the indicators used in this research. Additionally, the lack of people's willingness to shift to other parts leaving native areas impacted by landslides also increases the impact in the study area thereby the possibility of increasing the vulnerability. Moreover, analyzing and comparing the vulnerability obtained from the hazard mapping i.e. landslide mapping using GIS tool with the vulnerability extracted from the social method i.e. using LDCRP guideline is not convergent. For instance, most of the Satyawati RM is highly vulnerable from the susceptible map which differs from the vulnerable map prepared using LDCRP guidelines. This is due to the reason that landslide hazard mapping typically focuses on identifying areas that are susceptible to landslide based on causative factors like slope, geology, land use, distance from the road, rainfall, etc., while social vulnerability like LDCRP reveals the areas or wards that are proximal to the landslide whose ability to prepare for, respond to and recover from the hazards are impacted by the factors like demographic (population including disabled persons, children, senior citizens), socio-economic (low income and unemployment, economic loss, agricultural loss), lower environmental resources including knowledge, skill, capacity and technological factors not accounted by the hazard mapping. This illustrates that the degree of vulnerability of any area not only entirely depends upon their exposure to the hazard but also the socio-economic, environmental, demographic, and local knowledge. Thus, relying on only one approach cannot provide complete accessibility of the vulnerability. Integrating both methods allows for a complete vulnerability assessment addressing both the physical and socio-economic dimensions.

CONCLUSIONS

For the preparation of the landslide susceptible map, satellite imageries of the landslide from the Google Earth platform were used in the inventory process. Altogether 339 landslides were identified in the Badigad watershed which was divided into training data (80%) and testing data (20%). The testing data for this study was used for creating a prediction rate curve via ROC graph and determining the Area Under Curve value to validate the model. Weight of Evidence model (WoE) was used for the landslide susceptibility mapping. Based on the literature review, landslide-causing factors like slope, elevation, aspect, profile and plan curvature, relief, geological formation, distance from the road, distance from the river, land use, and rainfall are considered for landslide susceptibility mapping. The landslide susceptible map of the study area shows that 11% to 29% of the study area has very high to very low landslide susceptibility, whereas 26% has a medium, and 17 % has low landslide susceptibility. Satyawati Rural municipality of Gulmi is found to occupy the maximum landslide susceptible zones in this research. The validation of the model was done by using AUC, which states the model's prediction accuracy to be 70%. Vulnerability assessment of the Badigad watershed includes 5 municipalities and 20 wards showed that 1 of the wards of Chandrakot RM within the watershed is found to be at low vulnerability, 17 wards lying within the watershed were found under medium vulnerability to the landslide, and the other 2 wards were found to be highly vulnerable. The result obtained by analyzing and comparing the vulnerability from the physical method tool with the vulnerability extracted from the social method is not convergent.

ACKNOWLEDGEMENTS

We gratefully acknowledge the financial support received particularly from the Department of Environment, Government of Nepal funding munificently to carry out this dissertation task under the Study and Research Aid Program for fiscal year 2077/78. We also acknowledge Kiran Rayamajhi for his support in the fieldwork and Kumod Raj Lekhak for conducting the data analysis.

AUTHOR CONTRIBUTIONS

SB: Conceptualization, fieldwork, manuscript draft, reviewing, editing; MG: conceptualization, reviewing, and editing; PM: mapping, reviewing, and editing.

CONFLICTS OF INTEREST

All authors declared no conflicts of interest while publishing this paper.

DATA AVAILABILITY

All data of this research are with the corresponding author and if needed, these could be provided.

REFERENCES

Abedini, M., Ghasemyan, B., & Rezaei Mogaddam, M. H. (2017). Landslide susceptibility mapping in Bijar city, Kurdistan Province, Iran: a comparative study by logistic regression and AHP models. *Environmental Earth Sciences*, *76*, 1-14.

Acharya, K.K. (2018). Local governance restructuring in Nepal: From government to governmentality. *Dhaulagiri Journal of Sociology and Anthropology, 12*, 37-49. https://doi.org/10.3126/dsa

Acharya, T.D., Yang, I., & Lee, D. (2017). GIS-based landslide susceptibility mapping of Bhotang, Nepal using frequency ratio and statistical index methods. *Journal of the Korean Society of Surveying Geodesy Photogrammetry and Cartography, 35*(5), 357–364. https://doi.org/10.7848/ksgpc.2017.35.5.357

Aleotti, P., & Chowdhury, R. (1999). Landslide hazard assessment: summary review and new perspectives. *Bulletin of Engineering Geology and the Environment, 58*, 21-44. https://doi.org/10.1007/s10

Arrogante-Funes, P., Bruzón, A.G., Arrogante-Funes, F., Ramos-Bernal, R.N., & Vázquez-Jiménez, R. (2021). Integration of vulnerability and hazard factors for landslide risk assessment. *International Journal of Environmental Research and Public Health*, *18*(22), 11987. https://doi.org/10.3390/ijerp

Ayalew, L., & Yamagishi, H. (2005). The application of GIS-based logistic regression for landslide susceptibility mapping in the Kakuda-Yahiko Mountains, Central Japan. *Geomorphology, 65*(1-2), 15-31. https://doi.org/10

.1016/j.geomorph.2004.06.0

Banuzaki, A.S., & Ayu, A.K. (2021). Landslide vulnerability assessment using GIS and remote sensing techniques: a case study from Garut–Tasikmalaya road. *Conference Series: Earth and Environmental Science, 622*(1), 012005. https://doi.org/10.1088/1755-1315/622/1/012005

Baruwal, A. (2014). Disaster profile of Nepal. *Emergency and Disaster Reports, 1*(3), 3-49.

Bhattarai, D., Tsunaki, R., & Mishra, A.N. (2002). Water and Risk. In: Proceedings of Asia High Summit, ICIMOD, Kathmandu, Nepal.

Bonham-Carter, G.F. (1994). *Geographic Information Systems for Geoscientists; modeling with GIS*, Pergamon Press, Ottawa, Ontario, Canada.

Budha, P.B., Paudyal, K., & Ghimire, M. (2016). Landslide susceptibility mapping in eastern hills of Rara Lake, western Nepal. *Journal of Nepal Geological Society*, *50*(1), 125-131. https://doi.org/10.3126/jngs.v50i1.22872

Budha, P.B., Rai, P., Katel, P., & Khadka, A. (2020). Landslide hazard mapping in Panchase mountain of central Nepal. *Environment & Natural Resources Journal*, *18*(4), 387-399. https://doi.org/10.32526/ennrj.18.4.2020.37

Cannon, T. (2006). Vulnerability analysis, livelihoods and disasters. RISK21 - *coping with risks due to natural hazards in the 21st Century*, Liisa Roponen at UNU-WIDER, Helsinki, Finland.

Cao, Y., Wei, X., Fan, W., Nan, Y., Xiong, W., & Zhang, S. (2021). Landslide susceptibility assessment using the Weight of Evidence method: A case study in Xunyang area, China. *PLoS One, 16*(1), e0245668. https://doi.org/10.1371/journal.pone.0245668

Chen, Z., & Song, D. (2023). Modeling landslide susceptibility based on convolutional neural network coupling with metaheuristic optimization algorithms. *International Journal of Digital Earth, 16*(1), 3384-3416. https://doi.org/10.1080/17538947.2023

Chen, Z., Liang, S., Ke, Y., Yang, Z., & Zhao, H. (2019). Landslide susceptibility assessment using evidential belief function, certainty factor, and frequency ratio model at Baxie River basin, NW China. *Geocarto International*, *34*(4), 348-367. https://doi.org/10.1080/10106049.2017.1404143

Coburn, A., Sspence, R. J. S., and Pomonis, A. (1994). *Vulnerability and risk assessment*, Cambridge Architectural Research Limited, The Oast House, Malting Lane, Cambridge, United Kingdom

Corominas, J., van Westen, C., Frattini, P., Cascini, L., *et al.* (2014). Recommendations for the quantitative analysis of landslide risk. *Bulletin of Engineering Geology and the Environment, 73*(2), 209-263. https://doi.org/10.1007/s10064-013-0538-8

Cruden, D.M. (1991). A simple definition of a landslide. Bulletin of International Association Engineering Geology, 43(1), 27-29. https://doi.org/10.1007/BF02590167

Cutter, S.L. (1996). Vulnerability to environmental hazards. Progress in Human Geography, 20(4), 529-539. https://doi.org/10.1177/030913259602000407d10030315

Dahal, R.K. (2012). Rainfall-induced landslides in Nepal. *International Journal of Erosion Control Engineering*, *5*(1), 1-8. https://doi.org/10.13101/ijece.5.1

Dahal, R.K. (2017). Landslide hazard mapping in GIS, *Journal of Nepal Geological Society*, 53 (0), pp. 63-91. https://doi.org/10.3126/jngs.v53i0.23808

Dahal, R.K., & Hasegawa, S. (2008). Representative rainfall thresholds for landslides in the Nepal Himalaya, *Geomorphology,* 100 (0), pp. 429-443. https://doi.org/10.1016/j.geomorph.2008.01.014

Dahal, R. K., Hasegawa, S., Bhandary, N. P., Poudel, P. P., Nonomura, A., & Yatabe, R. (2012). A replication of landslide hazard mapping at catchment scale. *Geomatics, Natural Hazards and Risk*, *3*(2), 161-192. https://doi.org/10.1080/19475705.2011.629007

Dahal, R.K. (2012). Rainfall-induced landslides in Nepal. *International Journal of Erosion Control Engineering, 5*(1), 1-8. https://doi.org/10.13101/ijece

Dahal, R.K. (2017). Landslide hazard mapping in GIS. *Journal of Nepal Geological Society, 53*, 63-91. https://doi.org/10.3126/jngs.v53i0.23808

Dahal, R.K., Hasegawa, S., Bhandary, N.P., Poudel, P. P., Nonomura, A., & Yatabe, R. (2012). A replication of landslide hazard mapping at catchment scale. *Geomatics, Natural Hazards and Risk, 3*(2), 161-192. https://doi.org/10.1080/19475705.2011.6290

Dangol V., Upreti B.N., Dhital M.R., Wagner A., Bhattarai, T.N., Bhandari, A.N., Pant, S.R., & Sharma, M.P. (1993). Engineering geological study of a proposed road corridor in eastern Nepal. *Bulletin of the Department of Geology*, *3*(1), 91-107.

Devkota, K.C., Regmi, A.D., Pourghasemi, H.R., Yoshida, K., Pradhan, B., Ryu, I.C., ... & Althuwaynee, O.F. (2013). Landslide susceptibility mapping using certainty factor, index of entropy and logistic regression models in GIS and their comparison at Mugling–Narayanghat road section in Nepal Himalaya. *Natural Hazards, 65*, 135-165. https://doi.org/10.1007/s11069-012-0347-6

Dou, J., Bui, D.T., Yunus, A.P., Jia, K., Song, X., Revhaug, I., Xia, H., & Zhu, Z. (2015). Optimization of causative factors for landslide susceptibility evaluation using remote sensing and GIS data in parts of Niigata, Japan. *PloS One, 10*(7), e0133262. https://doi.org/10.1371/journal.pone.0133262

Füssel, H.M. (2007). Vulnerability: a generally applicable conceptual framework for climate change research. Global Environmental Change, 17, 155–167. https://doi.org/10.1016/j.gloenvcha.2006.05.002

Gerrard, J., & Gardner, R. (1999). Landsliding in the Likhu Khola drainage basin, middle Hills of Nepal. *Physical Geography, 20*(3), 240-255. https://doi.org/10.1080/02723646.1999.10642678

Getachew, N., & Meten, M. (2021). Weights of evidence modeling for landslide susceptibility mapping of Kabi-Gebro locality, Gundomeskel area, Central Ethiopia. *Geoenvironmental Disasters, 8*(1), 1-22. https://doi.org/10.1186/s40677-021-00177-z

Ghimire, M. (2011). Landslide occurrence and its relation with terrain factors in the Siwalik Hills, Nepal: Case study of susceptibility assessment in three basins. *Natural Hazards, 56*(1), 299–320. https://doi.org/10.1007/s11069-010-9569-7

Glade, T. (2003). Vulnerability assessment in landslide risk analysis. *Die Erde, 134*(2), 123-146.

Hasegawa, S., Dahal, R.K., Yamanaka, M., Bhandary, N.P., Yatabe, R., & Inagaki, H. (2008). Causes of large-scale landslides in the Lesser Himalaya of central Nepal. *Environmental Geology, 57*, 1423–1434. https://doi.org/1

0.1007/s00254-008-1420-z

Hearn, G., Petley, D., Hart, A., Massey, C., & Chant, C. (2003). Landslide Risk Assessment in the Rural Sector: Guidelines on Best Practice. UK Department for International Development (DFID).

Kayastha, P. (2012). Application of fuzzy logic approach for landslide susceptibility mapping in Garuwa sub-basin, east Nepal. *Frontiers of Earth Science, 6*(4), 420–432. https://doi.org/10.1007/s11707-012-0337-8

Kayastha, P., Dhital, M. R., & De Smedt, F. (2012). Landslide susceptibility mapping using the weight of evidence method in the Tinau Watershed. Nepal, *Natural Hazards, 63*(2), pp. 479–498. https://doi.org/10.1007/s11069-012-0163-z

Kayastha, P., Dhital, M. R., & De Smedt, F. (2013). Application of the analytical hierarchy process (AHP) for landslide susceptibility mapping: A case study from the Tinau watershed, west Nepal. *Computers & Geosciences*, 52 (0), 398–408. https://doi.org/10.1016/j.cageo.2012.11.003

Kayastha, P., Dhital, M.R., & De Smedt, F. (2012). Landslide susceptibility mapping using the weight of evidence method in the Tinau Watershed, Nepal. Natural Hazards, 63(2), 479–498. https://doi.org/10.1007/s11069-012-0163-z

Kayastha, P., Dhital, M.R., & De Smedt, F. (2013). Application of the analytical hierarchy process (AHP) for landslide susceptibility mapping: A case study from the Tinau watershed, west Nepal. *Computers & Geosciences, 52*, 398–408. https://doi.org/10.1016/j.c

Kharel, S. (2019). Local governance and rural development practices in Nepal. *Nuta Journal*, *6*(1-2), 84-94. https://doi.org/10.3126/nutaj.v6i1-2.23233

Lee, S., & Pradhan, B. (2007). Landslide hazard mapping at Selangor, Malaysia using frequency ratio and logistic regression models. *Landslides*, 4(1), pp. 33–41. https://doi.org/10.1007/s10346-006-0047-y

Li, Z., Nadim, F., Huang, H., Uzielli, M., & Lacasse, S. (2010). Quantitative vulnerability estimation for scenario-based landslide hazards. *Landslides, 7*(2), pp. 125–134. https://doi.org/10.1007/s10346-009-0190-3

Mersha, T., & Meten, M. (2020). GIS-based landslide susceptibility mapping and assessment using bivariate statistical methods in Simada area, northwestern Ethiopia. *Geoenvironmental Disasters, 7*(1), 1-22. https://doi.org/10.1186/s40677

Mihir, M., & Malamud, B. (2014). Identifying landslides using Google Earth, *Landslide Modeling and Tools for Vulnerability Assessment Preparedness and Recovery Management (LAMPRE)*, King's College, London.

Nohani, E., Moharrami, M., Sharafi, S., Khosravi, K., Pradhan, B., Pham, B.T., Lee, S., & Melesse, A. (2019). Landslide susceptibility mapping using different GIS-based bivariate models. *Water, 11*(7), 1402. https://doi.org/10.3390/w11071402

Nor Diana, M.I., Muhamad, N., Taha, M.R., Osman, A., & Alam, M.M. (2021). Social vulnerability assessment for landslide hazards in Malaysia: A systematic review study. *Land, 10*(3), 315. https://doi.org/10.3390/land10030315

Ojha, T.P. (2009). *Magnetostratigraphy, topography, and geology of the Nepal Himalaya: A GIS and paleomagnetic approach*. The University of Arizona.

Pamela, Sadisun, I.A., & Arifianti, Y. (2018). Weights of evidence method for landslide susceptibility mapping in Takengon, Central Aceh, Indonesia. *IOP Conference Series: Earth and Environmental Science*, 118, 012037. https://doi.org/10.1088/17551315/118/1/012037

Papathoma-Köhle, M., Neuhäuser, B., Ratzinger, K., Wenzel, H., & Dominey-Howes, D. (2007). Elements at risk as a framework for assessing the vulnerability of communities to landslides. Natural Hazards and Earth System Sciences, 7(6), 765-779. https://doi.org/10.5194/nhess-7-765-2007

Paudyal, K.R., & Maharjan, R. (2022). Landslide susceptibility mapping of the Main Boundary Thrust (MBT) region in Tinau-Mathagadhi Section of Palpa District, Lumbini Province. *Journal of Nepal Geological Society, 63*(01), 99-108. https://doi.org/10.3126/jngs.v63i01

Petley, D.N., Hearn, G.J., Hart, A., Rosser, N.J., Dunning, S.A., Oven, K., & Mitchell, W.A. (2007). Trends in landslide occurrence in Nepal. *Natural Hazards, 43*(1), 23-44. https://doi.org/10.1007/s110

Poudel, K., & Regmi, A.D. (2016). Landslide susceptibility mapping along Tulsipur-Kapurkot road section and its surrounding region using bivariate statistical model. *Journal of Nepal Geological Society, 50*(1), 83-93. https://doi.org/10.3126/jngs.v

Poudyal, C.P., Chang, C., Oh, H.J., & Lee, S. (2010), Landslide susceptibility maps comparing frequency ratio and artificial neural networks: a case study from the Nepal Himalaya. *Environmental Earth Sciences, 61*(5), 1049-1064. https://doi.org/10.1007/s12665-009-0426-5

Pradhan, A.M.S., & Kim, Y.T. (2016). Landslide susceptibility mapping of Phewa catchment using multilayer perceptron artificial neural network. *Nepal Journal of Environmental Science, 4*, 1-9. https://doi.org/10.3126/njes.v4i0.22718

Rabby, Y.W., & Li, Y. (2020). Landslide susceptibility mapping using integrated methods: a case study in the Chittagong hilly areas, Bangladesh. *Geosciences, 10*(12), 483-509. https://doi.org/10.3390/geosciences10120483

Rahman, G., Bacha, A.S., Ul Moazzam, M.F., Rahman, A.U., Mahmood, S., Almohamad, H., Al Dughairi, A.A., Al-Mutiry, M., Alrasheedi, M., & Abdo, H.G. (2022). Assessment of landslide susceptibility, exposure, vulnerability, and risk in Shahpur valley, eastern Hindu Kush. *Frontiers in Earth Science,* 10:953627. https://doi.org/10.3389/feart.2022.953627

Regmi, A., Yoshida, K., Pourghasemi, H.R., Dhital, M., & Pradhan, B. (2014). Landslide susceptibility mapping along Bhalubang – Shiwapur area of mid-western Nepal using frequency ratio and conditional probability models. *Journal of Mountain Science, 11*(5), 1266–1285. https://doi.org/10.1007/s11629-013-2847-6

Robinson, D.M., & DeCelles, P. (2014). Finding the Lesser Himalayan duplex in the Himalayan thrust belt of far-western Nepal amidst forests, villages, farms, and leeches. *Geological Field Trips in the Himalaya, Karakoram and Tibet*, *47*.

Roy, J., & Saha, S. (2019). Landslide susceptibility mapping using knowledge driven statistical models in Darjeeling District, West Bengal, India. *Geoenvironmental Disasters, 6*(1), 1-18. https://doi.org/10.1186/s40677-019-0126-8

Sarda, V., & Pandey, D.D. (2019). Landslide susceptibility mapping using information value method. *Jordan Journal of Civil Engineering, 13*(2), 335–348.

Sarkar, S., Kanungo, D.P., Patra, A.K., & Kumar, P. (2006). GIS-based landslide susceptibility mapping - a case study in Indian Himalaya, disaster mitigation of debris

flows, slope failures and landslides. Universal Academy Press, Inc. Japan, pp. 617-624.

Sato, H.P., & Harp, E.L. (2009). Interpretation of earthquake-induced landslides triggered by the 12 May 2008, M7. 9 Wenchuan earthquake in the Beichuan area, Sichuan Province, China using satellite imagery and Google Earth. *Landslides, 6*, 153-159. https://doi.org/10.1007/s10346-009-0147-6

Shrestha, H.K., Bhandary, N.P., & Yatabe, R. (2004). Trends in human life and economic losses from landslides and floods in Nepal, In Proceedings of 2nd International Seminar on Disaster Mitigation in Nepal, Kathmandu, November 2003.

Sifa, S.F., Mahmud, T., Tarin, M.A., & Haque, D.M.E. (2020). Event-based landslide susceptibility mapping using weights of evidence (WoE) and modified frequency ratio (MFR) model: A case study of Rangamati district in Bangladesh. *Geology, Ecology, and Landscapes, 4*(3), 222-235. https://doi.org/10.1080/2

Singh, S., Joshi, A., Sahu, A., Arun Prasath, R., Sharma, S., & Dwivedi, C.S. (2022). Himalayan Landslides–Causes and Evolution. In Kanga, S., Meraj, G., Farooq, M., Singh, S.K., & Nathawat (Eds.), *Disaster Management in the Complex Himalayan Terrains: Natural Hazard Management, Methodologies and Policy Implications* (pp. 33-42). Cham: Springer International Publishing. https://doi.org/10.1007/978-3-030-89308-8_3

Soeters, R., & Van Westen, C.J. (1996). *Slope instability recognition, analysis and zonation, Landslides: investigation and mitigation*. Transportation Research Board National Research Council Special Report, National Academy Press, Washington D.C., USA

Sumaryono, D.M., Sulaksana, N., & DasaTriana, Y. (2015). Weights of evidence method for Landslide susceptibility mapping in Tandikek and Damar Bancah, West Sumatra, Indonesia. *International Journal of Science and Research (IJSR)*, *4*(10), 1283-1290.

Terlien, M. T. J., Van Westen, C. J., & van Asch, T. W. J. (1995). Deterministic modeling in GIS-based landslide hazard assessment. In: Carrara, A., & Guzzetti, F. (Eds), *Advances in Natural and Technological Hazards Research, 57–77.* Doi:10.1007/978-94-015-8404-3_4

Thapa, P.B., & Esaki, T. (2007). GIS-based quantitative landslide hazard prediction modelling in natural hillslope, Agra Khola watershed, central Nepal. *Bulletin of the Department of Geology, 10*, 63-70. https://doi.org/10.3126/bdg.v10i0.1421

Turner, B.L., Kasperson, R., Matson, P., Mccarthy, J., Corell, R.W., Christensen, L., Eckley, N., Kasperson, J.X., Luers, A., Martello, M.L., Polsky, C., Puslipher, A., & Schiller, A. (2003). A framework for vulnerability analysis in sustainability science. *Proceedings of the National Academy of Sciences of the United States of America, 100*(14), 8074–8079. https://doi.org/10.1073/pnas.1231335100

Van Tien, P., Le Hong Luong, P.D., Sassa, K., Takara, K., Sumit, M., Nhan, T.T., Dang, K., & Duc, D.M. (2021). Mechanisms and modeling of the catastrophic landslide dam at Jure Village, Nepal. Journal of Geotechnical and Geoenvironmental Engineering, 147(11), 05021010. https://doi.org/10.1061/(ASCE)GT.1943-5606.0002637

Van Westen, C.J. (2002). *Use of weights of evidence modeling for landslide susceptibility mapping*. International Institute for Geoinformation Science and Earth Observation (ITC), Enschede, The Netherlands.

Van Westen, C.J., Castellanos, E., & Kuriakose, S.L. (2008). Spatial data for landslide susceptibility, hazard, and vulnerability assessment: An overview. *Engineering Geology, 102(*3-4), 112-131. https://doi.org/10.1016/j.enggeo.2008.03.010

Wang, L.J., Guo, M., Sawada, K., Lin, J., & Zhang, J. (2016). A comparative study of landslide susceptibility maps using logistic regression, frequency ratio, decision tree, weights of evidence and artificial neural network. *Geosciences Journal, 20*, 117-136. https://doi.org/10.1007/s12303-015-0026-1

Woodard, J.B., Mirus, B.B., Crawford, M.M., Or, D., Leshchinsky, B.A., Allstadt, K.E., & Wood, N.J. (2023). Mapping landslide susceptibility over large regions with limited data. *Journal of Geophysical Research: Earth Surface,* e2022JF006810. https://doi.org/10.1029/2022JF006810

Yagi, H., & Oi, H. (1993). Hazard mapping on large-scale landslides in Lower Nepal Himalayas. In *International conference and field workshop on landslides* (pp. 111-116).

Zhao, X., & Chen, W. (2020). Optimization of computational intelligence models for landslide susceptibility evaluation. *Remote Sensing, 12*(14), 2180. https://doi.org/10.3390/rs12142180

Zhu, A.X., Miao, Y., Wang, R., Zhu, T., Deng, Y., Liu, J., Yang, L., Qin, C.Z., & Hong, H. (2018). A comparative study of an expert knowledge-based model and two data-driven models for landslide susceptibility mapping. *Catena, 166*, 317-327. https://doi.org/10.1016/j.catena.2018.04.003

Zorgati, A., Wissem, G., Vali, V., Smida, H., & Essghaiem, G.M. (2019). GIS-based landslide susceptibility mapping using bivariate statistical methods. *Journal Open Geosciences, 11*(1), 708-726. https://doi.org/10.1515/geo-2019-0056